Computer simulation study of the mean forces between ferrous and ferric ions in water

ARTICLE *in* THE JOURNAL OF PHYSICAL CHEMISTRY · JULY 1992

Impact Factor: 2.78 · DOI: 10.1021/j100194a059

Reprinted from The Journal of Physical Chemistry, 1992, 96.

Computer Simulation Study of the Mean Forces between Ferrous and Ferric Ions in Water

Joel S. Bader[†] and David Chandler*

Department of Chemistry, University of California, Berkeley, Berkeley, California 94720
(Received: March 6, 1992)

With molecular dynamics and Monte Carlo trajectories, we have studied the potential of mean force between two iron ions in a periodically replicated simple point charge (SPC) model of liquid water. The results of these calculations are similar whether the primary cell contains 430 or 1022 water molecules. In contrast, the results depend significantly upon the treatment of the long-ranged forces. Specifically, if the long-ranged forces are truncated at half the box length (either discontinuously or with smooth splines), the potential mean force between Fe^{2+} and Fe^{3+} ions is nonmonotonic, exhibiting a powerful attraction at interionic distances, R, beyond 6 Å. If, however, Ewald sums are performed, the potential is monotonic and close to $zz'/\epsilon R$. Here, z and z' refer to the ionic charges, and $\epsilon \approx 70$ is the dielectric constant of SPC water.

1. Introduction

The structures of aqueous ionic solutions are pertinent to a variety of chemical and biological phenomena. The particular ionic system we consider herein is one that we have examined in our studies of aqueous ferrous–ferric electron transfer.[1-3] It contains two charged particles constructed to mimic Fe^{2+} and Fe^{3+} (or, with intermediate charges, $Fe^{2.5+}$ and $Fe^{2.5+}$). The two ions are solvated in a box with hundreds of simple point charge (SPC) molecules which model liquid water. The potential energy functions for this system, which is periodically replicated, are specified in ref 1. Figure 1 shows the local structure of one of the ions as it is bound to its six nearest-neighbor water molecules—the ligands.

Our specific interest in this paper is with the behavior of the interionic potential of mean force, $w(R)$. This function can be broken into two parts

$$w(R) = zz'/R + \Delta w(R) \tag{1}$$

where zz'/R is the interaction between two charges z and z' in vacuum. The solvation contribution to the potential of mean force is included in $\Delta w(R)$. We may estimate $\Delta w(R)$ from dielectric continuum theory:

$$w(R) \approx \frac{zz'}{\epsilon R} = \frac{zz'}{R} - \frac{zz'}{R}\left(1 - \frac{1}{\epsilon}\right) \tag{2}$$

[†] Current address: Department of Chemistry, Columbia University, New York, NY 10027.

0022-3654/92/2096-6423$03.00/0

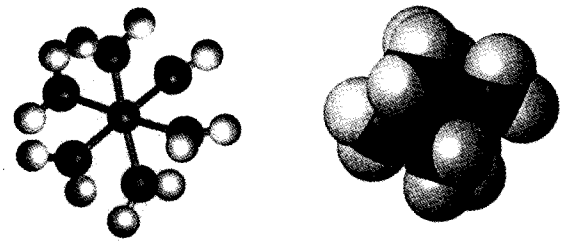

Figure 1. First solvation shell (ligand) structure of Fe^{3+} in water. As the simulations evolve, this structure fluctuates. The pictures show a typical equilibrium configuration. In the ball and stick representation, left, iron–oxygen bonds are drawn to aid the visualization. In the space filling representation, right, standard Pauling radii are assigned to the oxygen and hydrogen atoms. The oxygen–iron bond lengths are approximately 2 Å. The ligand structure of $Fe^{2.5+}$ and Fe^{2+} are very nearly the same. For example, the oxygen–iron bond is approximately 0.2 Å larger for $Fe^{2+}(H_2O)_6$ than it is $Fe^{3+}(H_2O)_6$.

At large R, for an infinite system, this formula is the correct asymptotic result for $w(R)$. For high dielectric solvents, eq 2 suggests that $\Delta w(R)$ is nearly as large in magnitude but opposite in sign from the direct interaction. In simulations, $\Delta w(R)$ is computed by averaging fluctuating forces. From eq 2, it therefore seems that these averages must be computed to high accuracy if one is to find physically meaningful results for the sum, $w(R)$.

In view of the near cancellation and concomitant sensitivity,[4] it might also be expected that simulation calculations of $w(R)$ will exhibit noticeable dependence upon the treatment of long-ranged forces. For this reason, we have carried out long runs and compared two different sets of simulations. In one, we truncate intermolecular interactions at half the periodic cell length. Despite longstanding concerns,[5] such truncations are often employed in simulations of aqueous solutions. When we use it, we find that the computed $w(R)$ is invariant to whether the truncations are done smoothly or discontinuously. (The latter we found more convenient to implement in Monte Carlo trajectories than in molecular dynamics simulations.) The results with truncated interactions are similar whether the primary simulation cell contains 430 water molecules or 1022 water molecules. Remarkably, however, the results of all these simulations with truncated potentials are very different from those obtained from an alternative set of calculations—simulations in which the long-ranged potentials are treated with Ewald sums.[6]

With truncated potentials, we find that $w(R)$ for two like sign iron ions is nonmonotonic, and it is strongly attractive for $R \gtrsim 6$ Å. In contrast, when we apply Ewald sums, we find the $w(R)$ is monotonic and purely repulsive. Our results are consistent with those of earlier workers who studied singly charged ions. Dang and Pettitt[7] and also Buckner and Jorgensen[7] employed simulations with truncated potentials and found significant attractions between pairs of Cl^- ions in water. Guârdia et al.[8] used Ewald sums and found a very weak attraction between pairs of Cl^- ions in water.

Our results for $w(R)$ are reported in section 3 and discussed in section 4. First, however, we turn to section 2, where we describe the methods we have employed.

2. Methods

Nearly all the results reported in the next section were computed by molecular dynamics at the constant temperature[9] of 300 K, with two ions and 430 SPC water molecules in a cubic primary box of volume (23.46 Å).[3] The density of water is thus close to 1 g/cm^3. A few calculations were carried out with a similar but larger system of volume (31.28 Å)^3 containing 1022 water molecules. In a classical system, $w(R)$ is independent of masses. We assigned a mass of 8 amu to the hydrogen nuclei and a mass of 16 amu to the oxygen nuclei. With these assignments, a relatively large integration time step could be used without destroying reasonable constancy of energy in the absence of the Hoover-Nosē thermostat.

After fixing the ions at a particular separation or range of separations with biasing potentials (see below), the system was equilibrated through heating and cooling cycles. For each of many different interionic configurations, statistics were collected for at least 5 ps after the equilibration runs were completed.

When truncating long-ranged potentials at a distance r_c, we use a smooth cubic spline of width Δ. For a given pair of molecules, the spline is one when the center of masses of the pair are separated by less than $r_c - \Delta$, and the spline is zero when the center-of-mass separation is larger than r_c. The intermolecular potentials are sums of site–site potentials multiplied by these splines. Except where otherwise noted, our calculations with truncated potentials used $\Delta = 0.5$ Å and $r_c = 11.73$ Å.

When performing Ewald sums, we employed the Gaussian width parameter (κ^{-1}, as defined in ref 5) of either 0.3 or 0.4 Å, and wave vector sums were truncated at a maximum wave vector magnitude of 2 Å^{-1}. Comparison tests convinced us that the Ewald sums were converged.

In performing Ewald sums with two ions in the system, we must imagine the presence of a uniform neutralizing background. Otherwise, an infinite Coulombic energy would be obtained. Even with the neutralizing background, however, were we to carry out Ewald sums with the asymmetric Fe^{2+}–Fe^{3+} system, a dipole would be replicated throughout space. The resulting torques would favor certain alignments of the Fe^{2+}–Fe^{3+} axis. To avoid this artifact, we have used Ewald sums only with a symmetric pair of $Fe^{2.5+}$ ions.

The computer simulations supplied data for the potential of mean force out to a largest value of R, termed R_{max}. The length L of a simulation box sets a limit on R_{max} for the last window; certainly, R_{max} should be smaller than $L/2$. Since $L/2$ was usually 11.73 Å, we did not attempt simulations past about 8 Å in this size box.

Simulations provide the slope of $w(R)$, not its absolute height. To integrate the slope, it is necessary to match the simulation results at R_{max} to a specific asymptotic form. The asymptotic form we have considered is the dielectric continuum limit, eq 2, with $\epsilon = 70$ for the static dielectric constant of SPC water.[10]

In some cases, we have obtained the potential of mean force between the two ions by integrating the solvent-averaged force felt by either of the ions. The ions were held at a fixed distance, and the mean force on each ion due to all the other particles in the system was determined. This procedure was repeated at a number of separations to give $F(R)$, the mean force as a function of ion–ion distance. Integration relates $F(R)$ to $w(R)$.

For some runs, the constraint on the interionic distance R was enforced by setting the forces on each ion to zero at each time step. For other runs, we introduced an extremely stiff spring between the ions. With the force constant of the spring set to 24 000 kcal/(mol Å^2), the root-mean-square deviation of the interionic distance was about 0.001 Å. The results from the stiff spring should be essentially the same that would be obtained with a holonomic constraint on the interionic separation.

The distance that the pair rotated or translated tended to be quite small over a few picoseconds of simulation; the ions tended to retain their initial orientation along a box axis. One specific box axis, perhaps the long diagonal, is presumably most favorable for the ions, but this detail was not investigated.

A second method of obtaining $w(R)$ is based on the relation

$$\exp[-\beta w(R)] \equiv g(R) \propto \langle \delta(\mathbf{R}_1 - \mathbf{R}_2 - \mathbf{R}) \rangle \qquad (3)$$

for instantaneous positions $\mathbf{R}_1$ and $\mathbf{R}_2$ of the two ions. The radial distribution function $g(R)$ was obtained through a series of window potentials $\Phi(R)$. The window potential added to the potential energy of a given configuration and favored sampling a certain region of R. The true $w(R)$ is related to the computed $g(R)$ by

$$w(R) = -k_B T \ln [g_\Phi(R)] - \Phi(R) - k_B T \ln \langle \exp[-\beta \Phi(|\mathbf{R}_1 - \mathbf{R}_2|)] \rangle \qquad (4)$$

The final term, different for each choice of $\Phi(R)$, but constant for a given window, was not determined directly from simulation. For the final window at the largest interionic separation, the constant was fixed by attempting to join $w(R)$ with the assumed asymptotic behavior, eq 2.

TABLE I: Parameters for the Window Potentials $\Phi(R) = k_\Phi(R - R_\Phi)^2/2$ That Were Used To Determine $w(R)$

$\langle R\rangle_\Phi$ (Å)[a]	k_Φ (kcal/(mol Å^2))	R_Φ (Å)	$\langle R\rangle_\Phi$ (Å)[a]	k_Φ (kcal/(mol Å^2))	R_Φ (Å)
4.3	23.9	3.0	5.5	7.17	4.5
4.5	19.1	3.0	6.0	11.9	5.5
4.9	23.9	4.0	6.5	4.78	5.5
5.0	11.9	3.5	7.0	4.78	6.0
5.0	19.1	4.0	7.5	2.39	6.0

[a] The average R observed in the window is $\langle R\rangle_\Phi$.

For the remaining windows at shorter distances, we employed a general technique which both avoided the necessity of matching each window and also saved the data from the windows on each side of an overlap. After $w(R)$ was calculated for a given window (to within the constant term), its derivative, dw/dR, equal to the negative of the mean force, was computed by numerical differentiation. Since the derivative of the constant term is zero, the mean force $F(R)$ was continuous across all the windows. Again, $F(R)$ for the final window should lie on top of the asymptotic result for the mean force.

Where the windows overlapped, the various values of $F(R)$ were averaged. A weighted average was employed, using $g_\Phi(R)$ as the weighting function for $F(R)$ from window $\Phi(R)$. In other words

$$F(R) = \frac{\sum_\Phi F_\Phi(R)\, g_\Phi(R)}{\sum_\Phi g_\Phi(R)} \tag{5}$$

and the resulting $F(R)$ was integrated with no need to match interior windows.

Two types of windows were employed in these simulations. The first type was a harmonic window

$$\Phi(R) = \tfrac{1}{2}k_\Phi(R - R_\Phi)^2 \tag{6}$$

used when $w(R)$ was relatively steep. The second type was a flat confining window which rose steeply at the edges

$$\Phi(R) = \begin{cases} \frac{1}{2}\, k_\Phi(R - R_\Phi + l/2)^2, & R - R_\Phi < -l/2 \\ 0 \quad -l/2 < R_\Phi < l/2 \\ \frac{1}{2}\, k_\Phi(R - R_\Phi - l/2)^2, & R - R_\Phi > l/2 \end{cases} \tag{7}$$

This type of window was effective for interionic separations of 8 Å or more. At 7.5 Å or less, the flat window provided insufficient biasing to obtain good statistics.

The windows selected for the umbrella sampling were chosen to be about 0.5 Å apart and to have a root-mean-square deviation of the interionic separation of about 0.2 Å. The parameters for the harmonic windows, and the ionic separation each samples, are listed in Table I. The flat confining window is defined by the width of the flat region. We performed simulations at 8 and 8.5 Å with the flat window and set the width to 0.7 Å.

There is a trade-off between the size of each window and the sampling efficiency. Since the motion within each window is largely diffusive, several smaller windows sample a region more effectively than a single large window. The smaller windows must still be large enough to have some overlap with each other. Averaging $F(R)$ where windows overlap, rather than matching $w(R)$ itself between windows, avoids the traditional loss of statistics in the overlap region and thus increases the efficiency of the sampling.

3. Results

3.1. With Truncated Interactions. The main set of simulations with truncated interactions considered Fe^{2+} and Fe^{3+} ions in a box of side 23.46 Å. The interactions were truncated at 11.73 Å with a 0.5-Å spline. Each calculation of the potential of mean force using these interactions yielded the same general result. As noted in the Introduction, we found a large attraction between the two ions. The minimum of the deep attractive well is at roughly 6 Å. As the ions move 1 Å in either direction, $w(R)$ increases by about $8k_BT$. The results of umbrella sampling about this minimum are shown in Figure 2. Its vertical placement on the graph is somewhat arbitrary since $w(R)$ computed with truncated interactions does not approach the anticipated asymptotic behavior at large R.

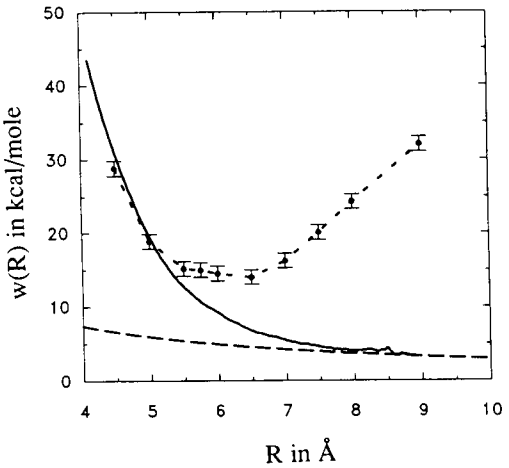

Figure 2. The potential of mean force, $w(R)$, for Fe^{2+}–Fe^{3+} (circles) and for $Fe^{2.5+}$–$Fe^{2.5+}$ (solid line) in water. The former is computed from simulations with truncated interactions. The latter is computed from simulations with Ewald sums. The dashed line is the dielectric continuum potential of mean force, $(2.5e)^2/R\epsilon$, with $\epsilon = 70$. The error bars are ±1 standard deviation. Error estimates for the solid line are of similar size (see Figure 3).

The outstanding feature of the $w(R)$ from truncated interactions, the large attractive well, was confirmed by a sequence of simulations. In one set, the ions were equilibrated near the minimum in the potential of mean force using a constraining potential. When the constraint on the ions was removed, the ions remained roughly 6 Å apart.

In a further test, the system wsa equilibrated with the ions 9 Å apart. Following the equilibration, the constraint was removed and the dynamics followed for a picosecond. In each of five trials, the ions moved closer to each other, on average by about 0.5 Å, as the simulation proceeded.

As the 432-particle simulation did not approach the expected asymptotic form of $w(R)$ for large R, further simulations were performed using a box 31.28 Å on a side with 1022 water molecules and the two ions. In this case, a 0.5-Å spline brought the interactions to zero smoothly at 15.64 Å. At an interionic separation of 10 Å, the mean force between the ions was still attractive. In the larger system, the size of the attractive force was 7 ± 1.5 kcal/(mol Å) at this distance.

To test whether the spline itself was in some way responsible for the ionic attraction, the length of the spline was changed. The ions in these simulations each bore a charge of 2.5+. When a 1-Å spline replaced the 0.5-Å spline, the ions still moved from an initial separation of 6.3 Å to a final separation of 5.4 Å over 4 ps of molecular dynamics. At this point the length of the spline was decreased to 0.1 Å and then to 0.02 Å; the ions remained within 0.5 Å of 5.4 Å.

A finite spline distance is required for energy conservation in the molecular dynamics simulation. To investigate the system with a vanishing spline, Monte Carlo simulations were employed. The standard Metropolis algorithm was used. All the interactions in the MC simulations were truncated abruptly at $L/2$. The ions, initially at 5.7 Å, remained within 0.2 Å of 5.7 Å throughout 16 000 passes, consistent with a local minimum in $w(R)$.

In summary, simulations using spherically truncated pair potentials display a large attractive well between the ions. The potential of mean force does not approach the asymptotic dielectric continuum form.

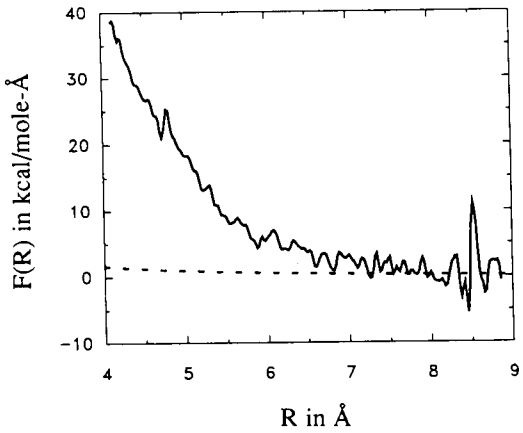

Figure 3. Mean force between two $Fe^{2.5+}$ particles in water computed from simulations by employing Ewald sums. Statistical uncertainties can be inferred from the roughness of the curve. The dashed line is the dielectric continuum mean force for the finite system, $[(2.5e)^2/\epsilon][R^{-2} - (L/2)^{-2}]$, with $\epsilon = 70$.

3.2. With Ewald Sums. As noted in section 2, we can avoid difficulties with Ewald sums for a unit cell with a permanent dipole by simulating a system with two identical ions, each of charge 2.5+. The structure and pertinent energetics of the $Fe^{2.5+}$–$Fe^{2.5+}$ system are very nearly the same as those for the asymmetric Fe^{2+}–Fe^{3+} system. Therefore, the behavior of $w(R)$ for two $Fe^{2.5+}$ ions should be indicative of that for the Fe^{2+}–Fe^{3+} pair.

The primary cell for the simulations with Ewald sums was 23.46 Å on a side, and 430 water molecules were included. The potential of mean force for these ionic charges with Ewald sums is shown in Figure 2. As seen from that graph, the ions repel each other, and the potential of mean force joins smoothly with the expected asymptotic limit. The potential is derived by numerically integrating the computed mean force. The latter is graphed in Figure 3, where the roughness of the curve provides a measure of the statistical uncertainties in our results. To within our uncertainties, the computed potential of mean force is perfectly fit for $R \gtrsim 4.5$ Å by

$$w(R) = zz'/\epsilon R + (24.3 \text{ kcal/mol}) \exp[-(R - 4.5 \text{ Å})/0.85 \text{ Å}] \quad (8)$$

with $z = z' = 2.5e$ and $\epsilon = 70$.

As a test of the repulsion, the $Fe^{2.5+}$ ions were released to move freely following equilibration at 5.5 Å. They moved to 7 Å within the first picosecond of simulation and continued to move apart as the simulation continued.

Unlike the potential of mean force generated using truncated interactions, there is no minimum in $w(R)$ for all the values of R examined, from 4 to 9 Å. It is possible that closer than 4 Å there is a local minimum in which a single water molecule serves as a ligand for each ion. Based on our simulation results for $w(R)$ at 4 Å, however, the energy barrier to reach such a configuration is at least 45 kcal/mol. The prohibitive energy cost makes it unlikely that such configurations could be important; the ligand shell remains intact for essentially all room temperature processes.

In Figure 3, the simulation forces are compared with the mean force from the dielectric continuum approximation

$$F(R) = (zz'/\epsilon)\left[\frac{1}{R^2} - \frac{1}{(L/2)^2}\right] \quad (9)$$

The constant, $(zz'/\epsilon)(L/2)^{-2}$, which is 0.2 kcal/(mol Å) in this case, is subtracted because the mean force between the two equally charged ions is zero by symmetry when the pair are separated by half the box length, $L/2$.

Beyond about 7 Å, the simulation mean force agrees with the dielectric continuum limit within statistical uncertainties. At smaller interionic separations, short-range repulsions cause the mean force to increase far above the dielectric continuum form.

TABLE II: The Mean Force $F(R)$ between Two $Fe^{2.5+}$ Particles a Distance R Apart[a]

	mean force (kcal/(mol Å))		
R (Å)	small system	large system	$z^2/\epsilon R^2$
5.5	9.8 (1)	10.7 (2)	0.98
8	0.4 (3)	1 (1)	0.46

[a] The small system contained 430 water molecules; the large system contained 1022. The dielectric continuum limit is $z^2/\epsilon R^2$. The mean force at 8 Å is an average over forces from 7.6 to 8.4 Å for the small system and from 8.1 to 8.9 Å for the large system. Error estimates (parentheses) are 1 standard deviation.

To test the dependence of the potential of mean force on system size, Ewald sums were performed for a larger system of 1024 particles in a box of side 31.28 Å. The mean force of this larger system was compared to the mean force from the smaller 432-particle system. The mean forces at an ionic separation of 5.5 Å and close to an 8-Å separation are listed in Table II. At 5.5 Å, the mean force for the small system is less repulsive than that of the large system by 0.9 kcal/(mol Å). The difference is 10% of the total force of 10 kcal/(mol Å).

The periodic images in Ewald sums might be responsible for the increase in the repulsive force for the larger simulation box. As ions in the principal unit cell move away from each other, they move closer to image ions in adjacent boxes. The direct force between the ions is consequently smaller for a smaller box, where the image ions are closer. In the 23.46-Å box, for example, ions on a box axis can be only 11.73 Å apart; in the larger box, they can be up to 15.64 Å apart. By symmetry, the direct force between the ions is zero when the pair in the central box are $L/2$ apart. Thus, the direct force goes to zero faster for the smaller box size.

At 5.5 Å, for instance, the direct force between the ions is 64.3 kcal/(mol Å) in the small box and 66.9 kcal/(mol Å) in the large box. For comparison, the force for the pair of ions neglecting the images is 68.6 kcal/(mol Å). The differences in the direct force in the small and the large system, 2.6 kcal/(mol Å), seems partially responsible for the difference in the mean force between the small and large systems. It is possible that dielectric screening reduces the magnitude of the difference to the 0.98 kcal/(mol Å) that we have computed.

4. Discussion

The results found with the Ewald sum prediction are physically reasonable. They agree with dielectric continuum estimates for $w(R)$ when the first solvation shells of the ions are separated by a distance of about a single water molecule. Doubling the system size affects details of the exact size of the mean force, but the doubling does not change the qualitative form of the mean force. In contrast, the strong attraction between the ions predicted using spherical truncation seems unphysical and is undoubtedly an artifact of the truncated interactions.

Competing finite size effects cause the difference between the Ewald sum and truncation results. Both Ewald sums and truncation produce a reaction field for a finite system that is smaller in magnitude than the reaction field, or solvation energy, of a truly infinite system. If this difference in solvation energy were independent of ionic separation, then the Coulombic screening in the finite system would be less than that of an infinite system, and the potential of the mean force would be more repulsive than in an infinite system. But the difference between the finite system reaction field and the infinite system reaction field does depend on the interionic separation. As the ions move further apart, more of the favorable solvation energy is lost in the finite system than would be lost in an infinite system. The net result is an attraction between the ions. For Ewald sums, the difference between the finite system and infinite system reaction fields seems not to depend as strongly on interionic separation. Consequently, the potential of mean force from Ewald sums is purely repulsive.

The water molecules most directly affected by truncation versus Ewald sums, and hence those responsible for the difference in the form of $w(R)$, are the ones located near the faces of the simulation

TABLE III: Electric Potential at an Ion in a Simulation of $Fe^{2.5+}$–$Fe^{2.5+}$ [a]

	electric potential at $Fe^{2.5+}$ (kcal/(mol e))		
	interionic separation		
solvent region	5.5 Å	8.5 Å	change
ligands, T	−215.3	−207.6	7.7
ligands, ES	−214.6	−206.8	7.8
sphere, T	−485.9	−425.1	60.8
sphere, ES	−428.5	−378.6	49.9
periodic array, T	−430.7	−381.2	49.5
periodic array, ES	−394.9	−353.3	41.6

[a] The configurations were sampled from trajectories generated with either truncated potential (T) or Ewald sums (ES) boundary conditions. Ligands refers to the 12 waters in the first solvation shell, sphere refers to the waters within 11.73 Å of either ion, and periodic array includes all the water images, i.e., an Ewald sum. Possible statistical errors of each entry are less than 0.5 kcal/(mol e).

unit cell. (Here we imagine that the center of the simulation box is midway between the ions.) With truncation, waters at the faces interact with one ion in the central unit cell and also with an ion image in a neighboring unit cell. The solvation energy from these waters is much less than that from waters which interact only with the ions in the center unit cell. As the ionic separation increases, a greater number of water molecules interact with one ion in the central unit cell and a second ion in an image cell. Thus, as the separation increases, an increasing fraction of the solvation energy is lost as well. With Ewald sums, the loss of solvation energy is not as dependent on interionic separation as it is with truncation. Under Ewald sums, each water molecule always experiences the potential from each of the ions and its images. Thus, for any given distance, the solvation energy for an ion in the central unit cell is less when computed with Ewald sums than it is when computed with truncation. As the ions move apart, however, less of the Ewald sum solvation energy is lost than is with truncation.

A quantitative comparison of the two boundary conditions with two equivalent $Fe^{2.5+}$ ions is made in Table III. The electric potential at an ion is shown for two interionic separations, 5.5 and 8.5 Å. The contribution to the electric potential from the ligands (not including the contributions from periodic images of ligand molecules) is seen to be independent of the boundary condition. Differences are observed when the total solvation energy is examined. For truncation boundary conditions, the solvation energy which governs the sampling includes contributions from waters within a sphere of 11.73 Å around each ion. This electric potential, listed in Table III as "sphere, T", decreases by 61 kcal/(mol e) as the ions move from 5.5 to 8.5 Å. In comparison, the corresponding decrease with Ewald sums, listed as "periodic array, ES", is only 42 kcal/(mol e).

Note that part of the difference between Ewald sums and truncation is due solely to the two boundary conditions summing different numbers of interactions. To complete our comparison of truncation and Ewald sums, we have taken trajectories produced using Ewald sums and recomputed the electric potentials using truncation. These results are entered as "sphere, ES" in Table III. We compare this electric potential to that calculated with truncation from trajectories produced with truncation boundary conditions. As our argument would indicate, the electric potential at an ion is less favorable for the Ewald sum configuration than for the configurations from the truncation trajectory. We have also taken the trajectories produced using truncation and recomputed the electric potential with Ewald sums. These results are listed as "periodic array, T" in Table III. Again, the Ewald sum electric potential computed from an Ewald sum trajectory has a less favorable electric potential at an ion than the electric potential from configurations from the truncation trajectory.

Incidentally, this argument suggests that, for different sign ions, the truncated interactions should lead to an excess *attraction* that is an artifact. Indeed, Huston and Rossky[11] have exhibited just this type of pathology. Huston and Rossky provide a qualitative explanation of the effect which is in accord with the argument we describe with Table III.

In summary, truncated long-ranged interactions can lead to substantial artifacts in the energetics governing the structure of ionic solutions. The net potential of mean force is the result of subtle cancellations. Hence, artifactual energetics may not necessarily lead to unphysical attractions in $w(r)$ for all systems with ions of the same sign. When the attraction does appear, however, it seems reasonable to expect it to persist to the largest values of R accessible from a finite-size simulation.[12] In contrast, Ewald sums lead to physically reasonable results which agree with the dielectric continuum potential of mean force for intermediate and large R. Ewald sums seem to be limited to the study of like charged ions. Other possibilities such as the reaction field method[13] might be more generally useful for asymmetric systems and worthy of investigation.

Acknowledgment. We are grateful to Jean-Pierre Hansen for informative discussions on the physics and computation of screening in Coulombic systems. Peter Rossky's comments on an earlier version of this paper have been helpful, too. This research was supported by the U.S. Department of Energy. The computations were performed on the University of California, Berkeley CRAY/XMP, and also on a Stellar GS1000 and a Stardent 3000 which were purchased and supported in part with grants from the National Science Foundation and the National Institutes of Health.

Registry No. Fe, 7439-89-6.

References and Notes

(1) Kuharski, R. A.; Bader, J. S.; Chandler, D.; Sprik, M.; Klein, M. L.; Impey, R. W. *J. Chem. Phys.* **1988**, *89*, 3248.
(2) Bader, J. S.; Chandler, D. *Chem. Phys. Lett.* **1989**, *157*, 501.
(3) Bader, J. S.; Kuharski, R. A.; Chandler, D. *J. Chem. Phys.* **1990**, *93*, 230.
(4) Dang, L. X.; Pettitt, B. M.; Rossky, P. J. *J. Chem. Phys.* **1992**, *96*, 4046.
(5) See: *NRCC Proceedings No. 9*, "The Problem of Long-Range Forces in Computer Simulation of Condensed Media"; Ceperley, D., Ed.; Lawrence Berkeley Laboratory: Berkeley, CA, 1980.
(6) See: Allen, M. P.; Tildesley, D. J. *Computer Simulation of Liquids*; Oxford University Press: Oxford, 1987; Section 5.5 and references cited therein.
(7) Dang, L. X.; Pettitt, B. M. *J. Phys. Chem.* **1990**, *94*, 4303. Buckner, J. K.; Jorgensen, W. L. *J. Am. Chem. Soc.* **1989**, *111*, 2507.
(8) Guàrdia, E.; Rey, R.; Padrò, J. A. *J. Chem. Phys.* **1991**, *95*, 2823.
(9) Nosé, S. *J. Chem. Phys.* **1984**, *81*, 511. Hoover, W. G. *Phys. Rev. A* **1985**, *31*, 1695.
(10) Watanabe, K.; Klein, M. L. *Chem. Phys.* **1989**, *131*, 157.
(11) In: Huston, S. E.; Rossky, P. J. *J. Phys. Chem.* **1989**, *93*, 7888; see especially Figure 1 and the discussion surrounding it.
(12) We note that Dang and Pettitt, ref 7, report one simulation calculation which exhibits both the strong attraction and the proper asymptotic limit. This result might merit reexamination. Buckner and Jorgensen's, ref 7, $w(r)$ exhibits the artifactual attraction, and as expected herein, it does not tend to the dielectric continuum result at large R.
(13) Barker, J. A.; Watts, R. O. *Mol. Phys.* **1973**, *26*, 789. See also: Barker, J. A. In ref 5 and references cited therein.